Meteoritics & Planetary Science 32, 123–133 (1997)

METEOMOD: A numerical model for the calculation of melting-crystallization relationships in meteoritic igneous systems

A. A. ARISKIN[1]*, M. I. PETAEV[2], A. A. BORISOV[1] AND G. S. BARMINA[1]

[1]Vernadsky Institute of Geochemistry and Analytical Chemistry, Russian Academy of Sciences, Moscow 117975, Russia
[2]Harvard-Smithsonian Center for Astrophysics, Cambridge, Massachusetts 02138, USA
*Correspondence author's e-mail address: ariskin@glas.apc.org

(Received 1996 May 10; accepted in revised form 1996 October 13)

Abstract–The METEOMOD model is a computer program designed to calculate melting-crystallization relationships in igneous systems compositionally similar to ordinary chondrites and basaltic achondrites. The core of METEOMOD is a set of empirically calibrated equations, called geothermometers, which describe equilibria between silicate melt and minerals such as olivine, orthopyroxene, pigeonite, augite, plagioclase, and metallic Fe in terms of pressure, temperature, and liquid compositions. The silicate mineral geothermometers are calibrated from a database containing the compositions of melts and minerals produced in melting experiments on 113 meteoritic and 141 synthetic systems. The metallic iron-silicate melt geothermometer is calibrated from a database of 396 melting experiments.

The Meteorite Melting Model or METEOMOD calculates crystallization temperatures and contents of major end members in mineral solid solutions with accuracies of ±10–15 °C and ±1–2 mol%, respectively. Input parameters for the program are (1) increment in crystallization degree; (2) one of 12 f_{O_2} buffers routinely used in petrology; (3) shift from the buffer in log units, if any; (4) a choice of equilibrium or fractional crystallization trajectory; (5) terminal crystallization degree; (6) contents of ten major elements in wt%; (7) a set of minor and trace elements in parts per million; (8) the number of initial compositions to be modeled in a single computation run. The output consists of a series of tables that list equilibrium temperatures, O fugacities, and proportions of melt and minerals and their compositions, as a function of the degree of crystallization.

The results of application of METEOMOD to modeling of melting-crystallization of the St. Severin LL chondrite are compared with the experimental data of Jurewicz *et al.* (1995).

INTRODUCTION

Igneous activity has resurfaced rocky terrestrial planets and differentiated their interiors throughout geologic time. The very old crystallization ages of most nonchondritic meteorites (exceptions being the Martian–SNC–and lunar meteorites), along with the detection of decay products of short-lived extinct nuclides in some of them (Lugmair *et al.*, 1996), show that the igneous differentiation of primitive parent bodies began soon after the condensation and agglomeration of the first solids in the solar nebula and was completed in a few tens of millions of years. The variety of differentiated meteorites known and the even greater abundance of 'igneous' asteroids in the modern asteroid belt (Gaffey *et al.*, 1993) suggest that magma generation and igneous fractionation were common in the early solar system.

It is generally believed that primary meteorite parent bodies had chondritic bulk compositions. Igneous activity in such a parent body would tend to differentiate the chondritic precursor material into a series of igneous rocks such as basalts, pyroxenites, dunites, *etc.*, with chemical and mineralogical compositions that depended upon the conditions of the igneous differentiation. As a result, initially more or less homogeneous parent bodies became radially and/or laterally stratified. Later dynamic evolution of the population of primary parent bodies, with mutual collisions and gravitational perturbations caused by the planets, delivered samples of these bodies to Earth as individual meteorites. These meteorites are not primitive, because their compositions are quite different from chondritic, but many of them still contain information on the chemistry, mineralogy, and mechanisms of differentiation of their parent bodies. This information can be decoded using general petrological techniques developed for the genetic interpretation of terrestrial igneous rocks.

The traditional approach to the study of igneous rock origins is to carry out melting experiments on natural samples of interest over a range of pressure, temperature, and O fugacity. Such experiments are designed to outline the P-T-f_{O_2} conditions under which the abundances and compositions of the melt and coexisting minerals produced in the experiment match those of the rock studied. A good example of such an approach is the experimental study of eucrites by Stolper (1977). Another approach to the study of igneous systems is to carry out melting/crystallization experiments in synthetic systems having various compositions (as opposed to natural rock compositions) in order to obtain information on phase equilibria as a function of the system composition. Both approaches provide important information on mineral stability fields, which is the basis of experimental petrology.

However, the systematic application of experimental petrology techniques to meteorites is difficult. Part of the problem is the scarcity of experimental data on meteoritic igneous systems. Another, more serious, difficulty is caused by the complexity of melting-crystallization relationships in multicomponent silicate melts, which often precludes the direct application of experimental results obtained in one igneous system to another. Progress in igneous petrology over recent decades has come from the development of computer models that are designed to calculate phase equilibria for a wide range of compositions from very primitive mafic magmas to basaltic and andesite-dacitic systems. Such programs are based on, and limited by, data from melting experiments, and may be considered as an empirical way to extend available experimental data to poorly studied systems and/or to a wider range of P-T-f_{O_2} conditions. Most of these models are designed to simulate crystal-melt fractionation in terrestrial basaltic magmas (Nielsen and Dungan, 1983; Frenkel and Ariskin, 1984; Ghiorso, 1985; Ariskin *et al.*, 1987, 1993b;

Nielsen, 1990; Weaver and Langmuir, 1990; Ghiorso and Sack, 1995) and have been successfully applied to selected volcanic series and mafic layered intrusions.

Several attempts also have been made to model the melting-crystallization relations of extraterrestrial igneous rock systems, such as lunar mare basalts (Longhi, 1987; Ariskin *et al.*, 1991), putative Martian magmas (Longhi and Pan, 1989), eucritic melts (Ariskin *et al.*, 1993a; Nazarov and Ariskin, 1993), primitive achondrites (Petaev *et al.*, 1994a,b,c), and shock-melted pockets in ordinary chondrites (Sack *et al.*, 1994). It is customary in all these models except that of Ariskin *et al.* (1993a) and Petaev *et al.* (1994a,b,c) to ignore equilibrium with a metallic phase, which limits their applicability to essentially metal-free igneous systems. Calculations have shown that precipitation of metallic Fe at extremely low f_{O_2} greatly increases the stability of low-Ca and high-Ca pyroxenes at the expense of olivine (Ariskin *et al.*, 1993a). This is also accompanied by a marked increase in the SiO_2 content of the melt equilibrated with metal. Recently these effects have been confirmed experimentally (Jurewicz *et al.*, 1995). Since chondrites (and probably the precursor materials of achondrites) contain variable but rather large amounts of metallic Fe, a model designed to calculate melting relations in primitive meteorite parent bodies clearly must include metal as one of the principal phases to be modeled. The purpose of this paper is to describe the Meteorite Melting Model, called hereafter METEOMOD, which was designed to simulate partial melting and crystallization in metal-bearing achondritic and chondritic systems at the low pressures conditions expected to have prevailed in primitive parent bodies. We will show that most of the experimental data on meteorites and lunar mare basalts, as well as a considerable part of the data for synthetic systems, can be used successfully to calibrate the METEOMOD over a wide range of compositions.

THERMODYNAMIC BACKGROUND

Crystallization of a primary homogeneous molten system may be thought of as a series of chemical reactions describing the progressive precipitation of solid phases from the melt as the system cools. For example, the equations

$$MgO\ (L) + 0.5SiO_2\ (L) = MgSi_{0.5}O_2\ (Ol) \qquad \text{Eq. (1)}$$

$$MgO(L) + SiO_2\ (L) = MgSiO_3\ (Op) \qquad \text{Eq. (2)}$$

describe the crystallization of two end members, forsterite into olivine solid solution (Eq. 1) and enstatite into orthopyroxene solid solution (Eq. 2), under condition when the melt is simultaneously saturated with both minerals. The two chemical components of the system involved in Eqs. 1 and 2, MgO and SiO_2, are partitioned among the three phases melt (L), olivine, and orthopyroxene. This partitioning can be described in terms of the equilibrium constants for Eqs. 1 and 2:

$$\ln K_e(\text{Eq. 1}) = \ln X_{Fo(Ol)} - \ln X_{MgO(L)} - 0.5\ln X_{SiO_2(L)} \qquad \text{Eq. (3)}$$

$$\ln K_e(\text{Eq. 2}) = \ln X_{En(Op)} - \ln X_{MgO(L)} - \ln X_{SiO_2(L)} \qquad \text{Eq. (4)}$$

where molar concentrations $X_{i(j)}$ approximate the activities of end members in mineral solid solutions and chemical components of the melt, and *Ke* is the equilibrium constant.

In a closed system, the amounts of chemical components partitioned among melt and solid phases[1] are linked by mass balance relationships, *e.g.*:

$$X_{MgO(bulk)} = X_{MgO(Fo)}X_{Fo(Ol)}F_{Ol} + X_{MgO(En)}X_{En(Op)}F_{Op} + X_{MgO(L)}F_L \qquad \text{Eq. (5)}$$

$$X_{SiO_2(bulk)} = X_{SiO_2(Fo)}X_{Fo(Ol)}F_{Ol} + X_{SiO_2(En)}X_{En(Op)}F_{Op} + X_{SiO_2(L)}F_L \qquad \text{Eq. (6)}$$

$$F_{Ol} + F_{Op} + F_L = 1 \qquad \text{Eq. (7)}$$

where F_j is the abundance (bulk concentration) of phase j in the system.

In a multicomponent system, similar chemical reactions and mass balance equations can be written for all end members of mineral solid solutions and all chemical components of the system. Then, if the numerical values of each K_e are known, the abundances and compositions of the melt and the minerals equilibrated with the melt can be calculated for any given set of intensive variables, such as pressure, temperature, and O fugacity.

Values of K_e can be computed directly from the measured compositions of the phases produced in melting/crystallization experiments or calculated from thermodynamic data using the relationship

$$\ln K_e = -\frac{(\Sigma G_{prod} - \Sigma G_{react})}{RT} \qquad \text{Eq. (8)}$$

where G_{prod} and G_{react} are the standard Gibbs energies of products and reactants, respectively, R is the universal gas constant, and T is the temperature in Kelvins.

Thermodynamic equilibrium in a multicomponent system having a particular set of intensive variables requires that the system components be distributed among a set of coexisting phases in a way, that yields the minimum possible total Gibbs energy for the system. There are two predominant ways to calculate the equilibrium phase assemblage in a partially molten system. One is based on an algorithm that minimizes the total Gibbs energy of the system using convex programming theory (Ghiorso, 1985). The other is the iterative solution of a system of nonlinear equilibrium equations that contain values of the equilibrium constants for each mineral-melt reaction (Frenkel and Ariskin, 1984; Ariskin *et al.*, 1993b). Both approaches are thermodynamically valid; the main difference between them is that the former minimizes the Gibbs energy of the system directly, whereas the latter uses Eq. (8) to link equilibrium constants to the Gibbs energy.

The common thermodynamic basis of these algorithms accounts for similar problems faced by the developers of mineral-melt equilibria models. First, there is a problem of formulation of the melt component activities that are needed to calculate both Gibbs free energies of silicate liquids (Ghiorso, 1985) and equilibrium constants for the reactions describing crystallization of minerals from the melts (Frenkel and Ariskin, 1984). Unfortunately, at present there is no working theory that correctly predicts activities of melt components for a wide range of compositions. For this reason, developers of computer models are forced to use simple, empirical descriptions of silicate melts that postulate the existence of some implausible molecules in the melts, such as SiO_2 and $NaAlO_2$ (Nielsen and Dungan, 1983) or Fe_2O_3 and Na_2SiO_3 (Ghiorso and Sack, 1995). Such empirical silicate-liquid models are employed by all computer programs that simulate mineral-melt equilibria, whatever mixing properties are assigned to silicate melts.

We draw readers' attention to this problem because there is a general impression that the employment of a regular-solution model in the MELTS program (Ghiorso and Sack, 1995) results in significantly better accuracy than that obtained by use of subideal solution models, as in MIXNFRAC (Nielsen and Dungan, 1983; Nielsen,

1990) or COMAGMAT (Ariskin *et al.*, 1993b). It is true that the thermodynamic description of both solid and liquid phases as nonideal solutions in the regular-solution model is more plausible than the subideal approach, which treats mineral solid solutions as ideal and attributes all nonideal effects to a liquid phase. However, both classes of models are based on the same database of experiments (see below), and regardless of the activity model used in calculations the accuracy of calculated temperatures and mineral compositions cannot be better than interlaboratory variabilities in experimental techniques and microprobe analytical uncertainties. Our experience in the field of mineral-melt equilibrium calculations has led us to conclude that a model calibrated with experimental data obtained in five to ten different laboratories can reproduce equilibrium temperatures measured in each particular experimental run with a precision of ~10–15 °C for 70–80% of the data. To achieve this degree of precision was the main requirement in the development of the METEOMOD program.

In this paper, we present a phase equilibrium model based on numerical solution of the system of nonlinear equations describing mineral-melt equilibria for olivine, augite, pigeonite, orthopyroxene, plagioclase, and metal, as well as mass balance constraints for 10 major and 20 trace elements (Frenkel and Ariskin, 1984). This technique was used first to develop a basic model, COMAGMAT, that simulates crystallization of multiply saturated magmatic melts step by step, as the total mode of crystals increases (Ariskin *et al.*, 1993b). The program calculates the liquid lines of descent of major components, the equilibrium proportions of melt and minerals, and the compositions of the latter. This model has been applied previously to a wide variety of terrestrial rocks, from primitive tholeiitic to calc-alkaline basalts. A specialized version of the program, LUNAMAG, was developed to model the crystallization of Fe-rich lunar basalts and eucrites (Ariskin *et al.*, 1991,1993a). In the METEOMOD program, we retain the general algorithm and the main features of both COMAGMAT and LUNAMAG; modifications needed to make the model applicable to achondritic and chondritic systems include recalibration of equations describing mineral-melt equilibria, and some improvements in the modeling of metal precipitation.

EMPIRICAL BASIS OF THE METEORITE MELTING MODEL

The cornerstone of METEOMOD is the set of empirical equations describing mineral-melt equilibria, so special care must be taken in calibrating them. To select the appropriate data from the numerous experimental studies available in the literature, we have used the INFOREX program, a sophisticated database designed to store and handle information on mineral-melt equilibria (for details see Meshalkin and Ariskin, 1996; Ariskin *et al.*, 1996). At present, the database contains information on over 6,300 experimental runs published in 168 experimental studies carried out since 1962. A substantial part of the database consists of results of melting experiments conducted with meteoritic samples, such as eucrites, shergottites and chondrites. These studies include a representative dataset of experimental glass compositions that rigorously defines the range of meteoritic compositions where the METEOMOD model can be applied with maximum accuracy.

Selection of Experimental Data for Meteorites

One-hundred-and-thirteen glass compositions produced in 1 atm meteorite melting experiments are in the INFOREX database. Based on their contents of rock-forming oxides, such as SiO_2, Al_2O_3, FeO, MgO, and CaO, these glasses were divided into three distinct groups (Table 1). Group I includes 66 eucrite-like compositions produced in experiments with ordinary eucrites (Stolper, 1977; Bartels and Grove, 1991) and shergottites (Stolper and McSween, 1979). The glasses produced by experimental melting of ordinary and carbonaceous chondrites at low O fugacities (Jurewicz *et al.*, 1991, 1993, 1995) also fall in this group. The 27 glasses of group II represent suggested parental magmas of SNC meteorites (Longhi and Pan, 1989) and howardites (Stolper, 1977). Group II also includes the most magnesian glasses produced by experimental melting of chondrites (Jurewicz *et al.*, 1993,1995). Group III in-

TABLE 1. Average composition of Fe enriched experimental glasses* obtained from melting experiments in meteoritic, lunar basalt, and synthetic silicate systems at 1 atm pressure.

System	Meteoritic						Lunar basalt and synthetic	
Group (*n*)	I (66)		II (27)		III (20)		IV (141)	
SiO_2	49.70	*(1.63)*	49.88	*(2.01)*	39.14	*(1.76)*	47.72	*(2.60)*
TiO_2	0.78	*(0.38)*	0.63	*(0.27)*	0.74	*(0.23)*	2.90	*(1.08, 120)*
Al_2O_3	12.25	*(1.07)*	7.32	*(2.02)*	12.00	*(1.20)*	10.57	*(1.87)*
FeO	19.54	*(1.83)*	20.90	*(3.27)*	25.58	*(4.71)*	21.39	*(3.28)*
MnO	0.37	*(0.23)*	0.51	*(0.17)*	0.19	*(0.05)*	0.15	*(0.14)*
MgO	6.42	*(1.09)*	10.54	*(1.76)*	6.67	*(1.39)*	5.85	*(2.12)*
CaO	10.26	*(0.89)*	9.58	*(2.91)*	13.70	*(2.63)*	11.48	*(2.79)*
Na_2O	0.57	*(0.46, 65)*	0.69	*(0.49, 23)*	0.67	*(0.49, 18)*	0.45	*(0.69, 111)*
K_2O	0.31	*(0.04, 3)*	0.16	*(0.03, 4)*	–		0.08	*(0.05, 55)*
P_2O_5	0.37	*(0.34, 19)*	0.08	*(0.02, 7)*	1.38	*(0.55, 20)*	–	
Cr_2O_3	0.28	*(0.11, 63)*	0.41	*(0.28, 27)*	0.08	*(0.05, 20)*	0.30	*(0.16, 103)*
Mg/(Mg + Fe)	0.369	*(0.050)*	0.473	*(0.056)*	0.317	*(0.009)*	0.328	*(0.098)*
Ca/(Ca + Al)	0.432	*(0.027)*	0.537	*(0.124)*	0.509	*(0.036)*	0.497	*(0.079)*

*All the experimental glass compositions were extracted from the INFOREX database (Ariskin *et al.*, 1996). The groups I, II, and III reprersent results of petrochemical classification of meteoritic glasses on the basis of SiO_2, Al_2O_3, FeO, MgO, and CaO contents. The group IV involves data obtained in lunar low-Ti basalt and synthetic systems. Standard deviations (1σ) for each component are given in the parentheses; the number of analyses for minor components is given after 1σ values.

cludes 20 angrite-like compositions produced in experients with the Allende and Murchison carbonaceous chondrites under oxidizing conditions (Jurewicz *et al.*, 1991, 1993).

The distinctive feature of all these experimental compositions is their enrichment in FeO; most of the meteorite glasses contain no less than 18 wt% FeO, so they can be treated as highly ferrous silicate systems, despite the elevated-to-high MgO contents of starting materials, especially in chondrites. Indeed, the values of mg# = Mg/(Mg + Fe) (molar) vary in the glasses from 0.228 to 0.567. This is an important point because detailed analysis of liquidus phase diagrams for lunar and terrestrial basalts (Longhi, 1991) has demonstrated that the phase diagram topologies for systems with high and low mg# may be different.

The meteoritic melts cover the range of experimental temperatures of 1350–1060 °C and are saturated with different mineral assemblages, such as Ol + Sp, Ol + Sp + LPyx (Op or Pg), and Ol + Sp + Pl + LPyx (mostly Pg). Shergottites display a wider stability field of high-Ca pyroxene (Stolper and McSween, 1979). Metal and/or sulfide was observed in the most reduced experiments with eucrites and ordinary chondrites (Stolper, 1977; Jurewicz *et al.*, 1993, 1995). For the sake of convenience, the phase equilibria and compositional data are summarized on the OLIV-PLAG-QTZ pseudoternary diagram projected from the CPX component (Fig. 1). The projection was done by converting the oxide weight percent into mole percent followed by calculation of fictive mineral components in terms of O units (Tormey *et al.*, 1987).

One of the main uses of a generalized liquidus diagram is to show the path that a derivative experimental liquid will follow upon melting of a chondritic precursor or crystallization of a chondritic melt. Figure 1 shows that the experimental data available to date permit the positions of the Pl-Ol and Ol-LPyx boundaries to be defined with confidence, but the assumed stability field of quartz is marked by only one experimental point. This diagram provides the most complete phase representation of the experimental dataset on meteorite melting available for calibration of the olivine-, plagioclase- and pyroxene-melt geothermometers. However, more than 30% of the data are characterized by short run durations (often <20 h), implying that complete equilibrium among minerals and melt might have not been achieved. Since careful calibration of geothermometers is crucial for METEOMOD, we have searched for additional experimental data in the INFOREX database.

In order to find data matching the range of meteoritic melt compositions and temperatures, a global search for experiments on terrestrial rocks, lunar basalts, and synthetic systems that meet certain criteria was conducted. The criteria included pressure (1 atm), temperature range (1050–1350 °C), run duration (>24 h), and glass composition parameters such as total alkalinity ($Na_2O + K_2O$ <3 wt%), TiO_2 content (<5 wt%, to exclude data on high-Ti lunar basalts), FeO content (>15 wt%), and Mg# (<0.55). Only 141 runs from 11 studies, mostly on lunar basalts, meet the criteria (Table 1). The OLIV-PLAG-QTZ projection of the selected glass compositions, including corresponding mineral-melt assemblages, is shown in Fig. 2. These data correspond to the main range of "meteoritic" peritectics and provide a more accurate location of the phase region where quartz is present on the liquidus. We

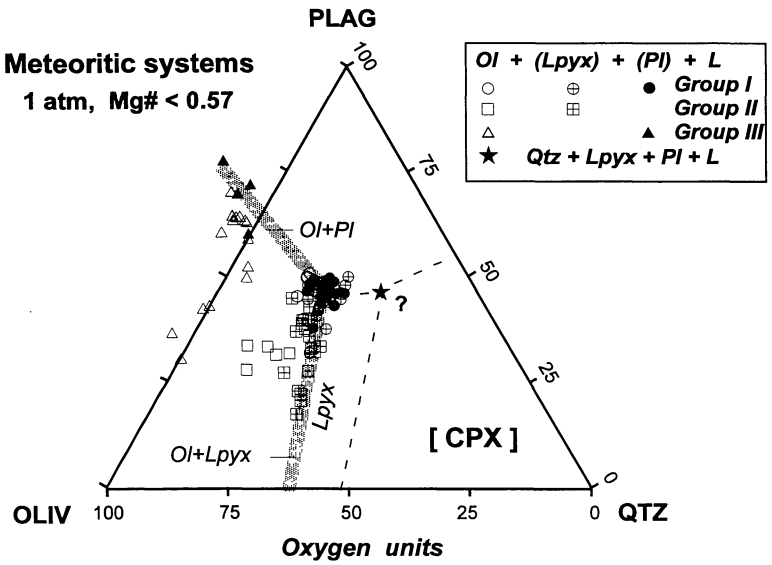

FIG. 1. Compositions of melts produced in 1 atm melting experiments on meteoritic samples. Data from the INFOREX database (Ariskin *et al.*, 1996) are projected from the CPX component by the technique of Tormey *et al.* (1987). Compositions of melts from three separate groups (Table 1), equilibrated with different mineral assemblages, are shown by different symbols. The data rigorously define the positions of the olivine-plagioclase and olivine–low-Ca pyroxene peritectics (broad shaded bands) in systems with mg# <0.57. Dashed lines outline the suggested stability field of quartz.

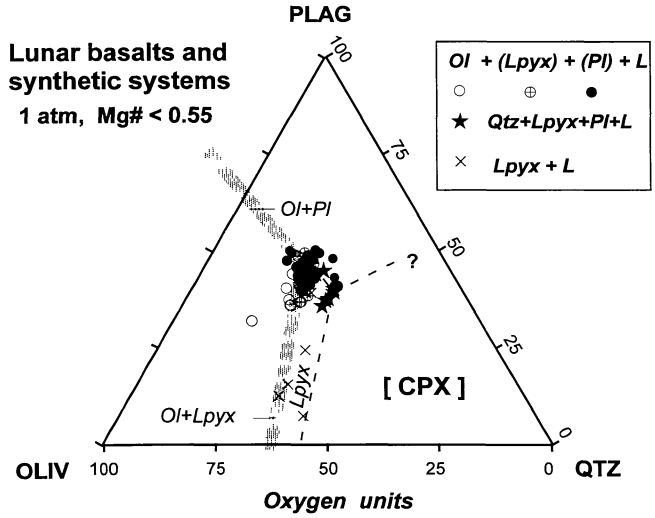

FIG. 2. Compositions of melts produced in 1 atm melting experiments on lunar basalts and synthetic samples. Data from the INFOREX database (Ariskin *et al.*, 1996) are projected from the CPX component by the technique of Tormey *et al.* (1987). Different symbols denote different mineral assemblages. The average composition of the melts is given in Table 1. The data on 'lunar' and synthetic systems are in good agreement with 'meteoritic' peritectics shown by shaded bands. Dashed lines show the stability field of quartz.

believe that the selected experiments on lunar basalts and synthetic systems (Fig. 2) combined with meteorite melting experiments (Fig. 1) constitute a representative dataset for the calibration of mineral-melt geothermometers.

Calibration of End-member-Melt Geothermometers

The core of METEOMOD is a set of empirically calibrated equations, called hereafter geothermometers, which describe mineral-melt equilibria in terms of pressure, temperature, and liquid compositions. The geothermometers can be constructed at a given

pressure for a selected set of coexisting mineral and glass compositions, if the equilibrium temperature is known. Calibration at a constant pressure is accomplished by a multiple regression in the form of a modified Arrhenius relation:

$$\ln K_{i(j)} = A_{i(j)} + \frac{B_{i(j)}}{T} + C_{i(j)} \ln R_{1(L)} + D_{i(j)} \ln R_{2(L)} \quad \text{Eq. (9)}$$

where $R_{1(L)}$ and $R_{2(L)}$ are atomic ratios of melt components, such as Si/O, Al/O, Al/Si, *etc.*, often called in petrologic literature melt structure-chemical parameters; the parameters $A_{i(j)}$, $B_{i(j)}$, $C_{i(j)}$, and $D_{i(j)}$ are the regression coefficients, and $K_{i(j)}$ is the equilibrium constant for the reaction that crystallizes end-member i in mineral j, *e.g.*, for forsterite in olivine (Eq. 1).

When the regression parameters are calculated, one can test the result for goodness of fit. The test procedure includes calculation of either $\ln K_{i(j)}$ or T for each liquid composition from the initial database and comparison of them with the experimental values. This procedure provides an independent estimate of the accuracy of the geothermometers; if they do not satisfy the required degree of precision of ~10–15 °C for 70–80% of the data, the calculations may be repeated for another combination of $R_{1(L)}$ and $R_{2(L)}$, until the best fit to the experimental data is obtained. Thus, an acceptable and easily controlled level of accuracy of geothermometers can be achieved by repeated calibrations. However, the latter are usually accurate only for a limited range of igneous system compositions (Nielsen and Dungan, 1983; Weaver and Langmuir, 1990).

Using the selected experimental dataset, five to six combinations of geothermometers in the form of Eq. (9) for 18 end members representing olivine, plagioclase, and pyroxene solid solutions were investigated. Mathematical processing of each combination was performed in two stages. In the first stage, the regression parameters of all geothermometers were calculated based on the entire dataset of coexisting mineral-melt compositions. Then, these regression parameters were used to calculate crystallization temperatures of all end members for each experimental melt. The experiments in which the difference between calculated and measured crystallization temperatures exceeded three standard deviations of the experimental temperature were considered unequilibrated. As a rule, in each set of calculations, two to four runs with calculated deviations of 30–60 °C from the experimental temperatures were excluded from the second stage processing. The latter was done using the same procedure as described above. Thus, the final sets of regression parameters were calculated based on a slightly reduced dataset. The regression parameters of all end-member geothermometers representing the best fits of the available experimental data are listed in Table 2.

Olivine–The selected olivine-melt experimental dataset includes 153 runs from 14 studies. These runs were conducted in the 1059–1350 °C temperature range, with >80% of data obtained at f_{O_2} corresponding to or below the iron-wüstite (IW) buffer; 50% of runs have duration ≥72 h. The calculated regression parameters for *Fa* and *Fo* show the strong effect of temperature and melt structure-chemical parameters on the optimal regression parameters (Table 2).

TABLE 2. Regression constants* for mineral-melt geothermometers calibrated in Fe enriched silicate systems at atmospheric pressure.

Component (n)	A [1/T]	B	C [$\ln R_{1(L)}$]†	D [$\ln R_{2(L)}$]†
Olivine‡				
Fa (149)	5951.8 *(104.4)*	–4.343 *(0.099)*	–0.206 *(0.058)*	–0.559 *(0.081)*
Mn-Ol§ (96)	6592.3 *(435.2)*	–6.161 *(0.358)*	–1.265 *(0.163)*	–
Fo (148)	5623.5 *(151.4)*	–3.992 *(0.143)*	–0.946 *(0.076)*	–0.798 *(0.112)*
Pigeonite				
Fs (99)	4628.5 *(233.7)*	–2.011 *(0.292)*	1.313 *(0.249)*	–1.219 *(0.190)*
Mn-Px§ (57)	5009.6 *(1217.9)*	–0.584 *(1.628)*	2.301 *(1.172)*	–
En (101)	7820.9 *(209.5)*	–4.378 *(0.259)*	–0.164 *(0.218)*	0.236 *(0.169)*
Wo (97)	15087.7*(1188.5)*	–15.910 *(1.449)*	–4.165 *(1.236)*	2.674 *(0.947)*
Orthopyroxene				
Fs (14)	4978.5 *(1143.2)*	–3.296 *(1.064)*	0.371 *(0.476)*	–1.014 *(0.568)*
Mn-Px§ (13)	2182.2 *(1397.4)*	0.202 *(1.300)*	2.153 *(0.579)*	–3.442 *(0.700)*
En (14)	6256.0 *(828.2)*	–2.481 *(0.771)*	0.743 *(0.345)*	–1.002 *(0.411)*
Wo (13)	13457.6 *(1276.4)*	–11.478 *(2.065)*	–0.587 *(1.690)*	–
Augite				
Fs (37)	8638.1 *(955.8)*	–2.654 *(1.000)*	3.464 *(0.443)*	–0.832 *(0.485)*
Mn-Px§ (9)	11083.3 *(1411.7)*	–5.367 *(2.016)*	2.528 *(1.604)*	–2.279 *(0.700)*
En (37)	10247.6 *(621.7)*	–6.601 *(1.646)*	–0.386 *(1.283)*	0.551 *(0.308)*
Wo (36)	589.1 *(0.578)*	0.054 *(0.414)*	–	0.572 *(0.275)*
Plagioclase				
Fe-An§ (50)	14202.7 *(2725.9)*	–10.235 *(2.403)*	–1.041 *(0.687)*	–
An (52)	10121.1 *(764.2)*	–5.515 *(0.646)*	–2.696 *(0.268)*	–
Ab (24)	17056.7 *(3689.0)*	–10.684 *(2.631)*	–	–

*The regression constants correspond to log of the mineral-melt equilibrium constants $K_{i(j)}$ calculated as per linear model (9): standard deviations (1σ) for each constant are given in the parentheses. Activities of the melt components were calculated using the two-lattice model of Nielsen and Dungan (1983), whereas the activities of mineral components were assumed to be equal to the fractions of cations in a single site (ideal solution).
†Melt structure-chemical parameters: $R_1 = Si/O$ [for *Ab* in *Pl*: $R_1 = (Si + Al)/O$], and $R_2 = Si/(Al + Si)$.
‡Also takes into account crystallization of the larnite end member, Ca_2SiO_4, from the melt, with the average value of the equilibrium constant being 0.033.
§Minor components: *Mn-Ol*, Mn_2SiO_4; *Mn-Px*, $MnSiO_3$; *Fe-An*, $FeSi_2Al_2O_8$.

Using the calibrated geothermometers, one can invert the calculations to obtain fayalite-melt and forsterite-melt equilibrium temperatures for each pair of olivine and liquid compositions from the initial dataset. The comparison between calculated and experimental temperatures shows that the absolute accuracies of fayalite and forsterite geothermometers are 8.0 °C and 11.4 °C, respectively. A graphic representation of the forsterite-geothermometer along with a frequency histogram of deviations between calculated and experimental temperatures is shown in Fig. 3. Minor components, such as Mn_2SiO_4 and Ca_2SiO_4, are known to have a small effect on the olivine saturation boundary, so we can expect that the modeling of olivine crystallization will reproduce olivine-melt experimental temperatures with an accuracy of 10–15 °C (see below).

Pyroxenes–The data on pyroxene-melt equilibria represent 10 experimental studies and include the compositions of 103 pigeonite-melt pairs (1050–1300 °C, 28 < t < 673 h), 14 orthopyroxene-melt pairs (1170–1350 °C, 48 < t < 168 h), and 38 augite-melt pairs (1062–1215 °C, 48 < t < 542 h). Most of the runs were conducted at low O fugacities, in the vicinity of IW buffer. Note that pigeonite crystallizes from a wide range of the selected melt compositions, whereas orthopyroxene was observed only in experiments with chondrites (Jurewicz *et al.*, 1995). Augite coexisting with melt was found in four experiments with lunar basalts and three experiments with shergottites (Stolper and McSween, 1979); the other 31 augite-melt pairs represent synthetic systems.

The calculated regression parameters for pigeonite, orthopyroxene, and augite geothermometers listed in Table 2 point to a strong dependence of the calculated constants on the Si/O and Al/(Al + Si) ratio in the melts. The most accurate geothermometers are derived for the enstatite end member, with the average temperature reproducibility being ±9.8 °C for pigeonite, ±4.9 °C for orthopyroxene, and ±8.7 °C for augite (see histograms in Fig. 3). Ferrosilite geothermometers are less accurate, providing an average accuracy of ±17.9 °C for pigeonite, ±8.6 °C for orthopyroxene, and ±18.2 °C for augite. Table 2 also displays a strong temperature dependence for the wollastonite end member in low-Ca pyroxenes; the effect of temperature on the calculated wollastonite regression parameters in high-Ca pyroxenes is insignificant.

Plagioclase–Compositions of 52 plagioclase-melt pairs were extracted from 8 studies, with only 13 pairs studied in experiments on meteorites. This dataset covers most of the range of plagioclase crystallization temperatures, 1075–1190 °C; all the experiments are characterized by sufficiently long run duration, with average t = 131 h. Most of the melts are also saturated with pyroxenes ± olivine; a few runs consist of Pl + L and Pl + Ol + L assemblages. The calculated regression parameters for three plagioclase end members listed in Table 2 show the strong effect of silicate liquid composition on the plagioclase-melt equilibrium. This is especially true for the dependence of anorthite regression parameters on the (Si + Al)/O ratio, which results in good accuracy for this geothermometer, the average temperature discrepancy being ±12.3 °C (Fig. 3). The Fe-anorthite ($FeAl_2Si_2O_8$) and albite geothermometers are less accurate; they reproduce experimental temperatures with an average accuracy of ±27.5 °C and ±16.3 °C, respectively. Note that in the case of albite, we imposed an additional constraint, taking into account only melts with sodium concentrations >0.1 wt%. This constraint is

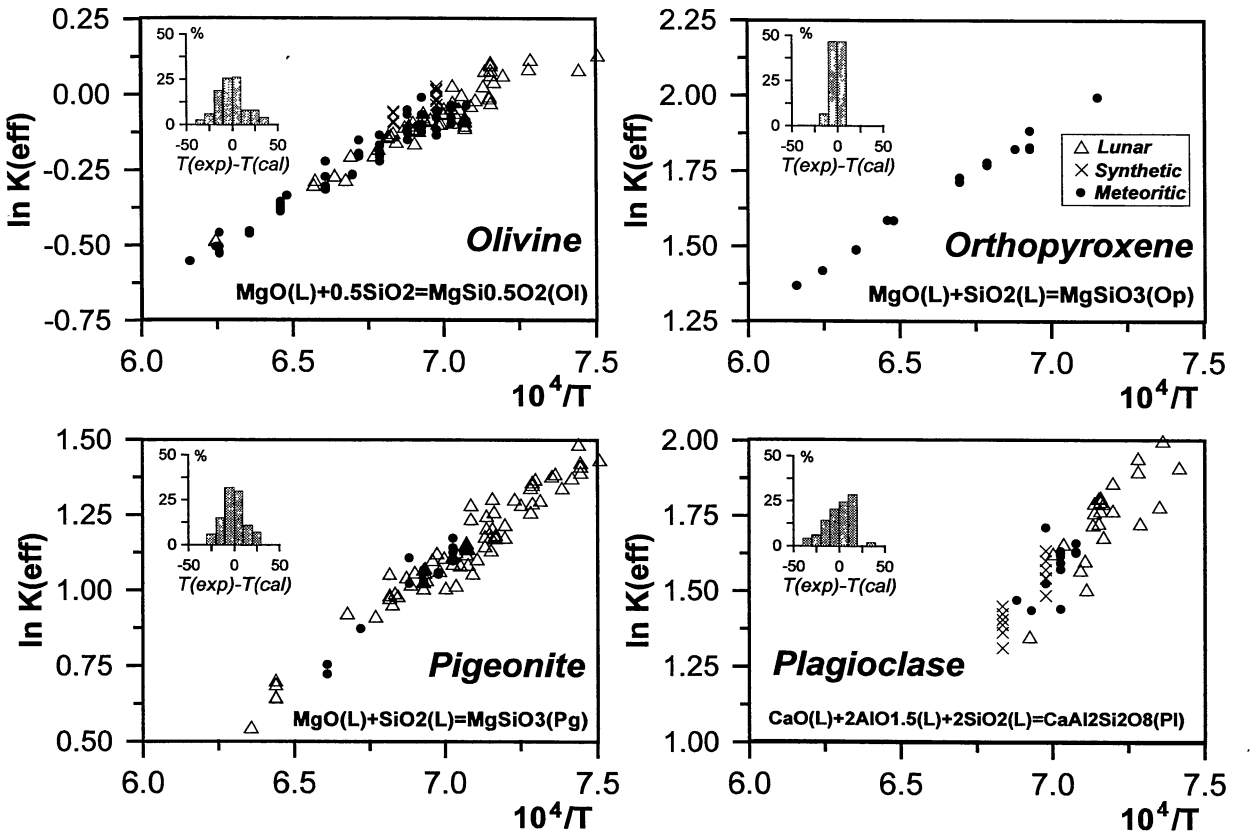

FIG. 3. Variations of logarithms of effective equilibrium constants ($\ln K_{eff}$) of mineral-melt reactions with temperature. Corrections for compositional effects on the equilibrium constant are calculated from the equation $\ln K_{eff} = \ln K_{i(j)} - C_{i(j)} \ln R_{1(L)} - C_{i(j)} \ln R2_{(L)}$. The regression parameters are from Table 2. The histograms show deviations (rel% of total number of runs) of calculated temperatures from those measured in experiments.

necessary to minimize the effect of possible analytical errors on the calculated regression parameters. On the basis of seven experimental points, we also calculated the average value of the equilibrium constant for the reaction describing crystallization of the orthoclase end member from the melt, $K_{Or} = 0.814 \pm 0.239$; this value was used in the development of a general model of plagioclase-melt equilibrium.

Testing Combined Mineral-Melt Geothermometers

The individual end-member geothermometers for each mineral solid solution (Table 2) can be combined into a single mineral geothermometer that calculates crystallization temperatures and compositions of mineral solid solutions as a function of liquid composition (Ariskin *et al.*, 1993b). For example, in the case of olivine, this can be done by combining the three equations for end-member geothermometers (Table 2) and the olivine stoichiometry equation:

$$X_{Fo(Ol)} + X_{Fa(Ol)} + X_{Mn_2SiO_4(Ol)} = 1 \qquad \text{Eq. (10)}$$

into a single system of equations, that constitute the combined mineral-melt geothermometer. Similar systems of equations can be formulated and solved for other minerals such as orthopyroxene, pigeonite, augite, and plagioclase.

To test the combined mineral geothermometers, we calculated crystallization temperatures and compositions of olivine, orthopyroxene, pigeonite, augite and plagioclase from the experimental melts used to calibrate the end-member geothermometers. The results, shown in Fig. 4, demonstrate both good reproducibility of experimental data and the internal consistency of the combined mineral geothermometers. The standard deviations of calculated crystallization temperatures of minerals are ±9.9 °C for olivine, ±3.2 °C for orthopyroxene, ±6.3 °C for pigeonite, and ±12.0 °C for plagioclase. The general improvement in accuracy of calculated crystallization temperatures of minerals as compared to those of individual end members (Fig. 3) is a well-known effect of the incorporation of individual end-member equations into a combined mineral geothermometer (Ariskin *et al.*, 1993b). The histograms in Fig. 4 also reveal good accuracy of modeled mineral compositions: ±0.96 mol% forsterite in olivine, ±0.93 mol% enstatite in orthopyroxene[2], ±1.53 mol% enstatite in pigeonite, and ±1.81 mol% anorthite in plagioclase. The observed internal consistency of both calculated temperatures and mineral compositions shows that a general model of phase equilibria based on empirical data for silicate minerals and melts can calculate melting-crystallization relationships in meteoritic systems with good accuracy.

Calibration of the Equation for Metal-Silicate Melt Equilibrium

The basic reaction describing the dissolution of Fe metal in a silicate melt is:

$$\text{Fe (met)} + 1/2\text{O}_2\text{ (gas)} = \text{FeO (liq)} \qquad \text{Eq. (11)}$$

with the equilibrium constant being

$$\log K(T) = \log a_{FeO(L)} - \log a_{Fe(Met)} - 0.5 \log f_{O_2} \qquad \text{Eq. (12)}$$

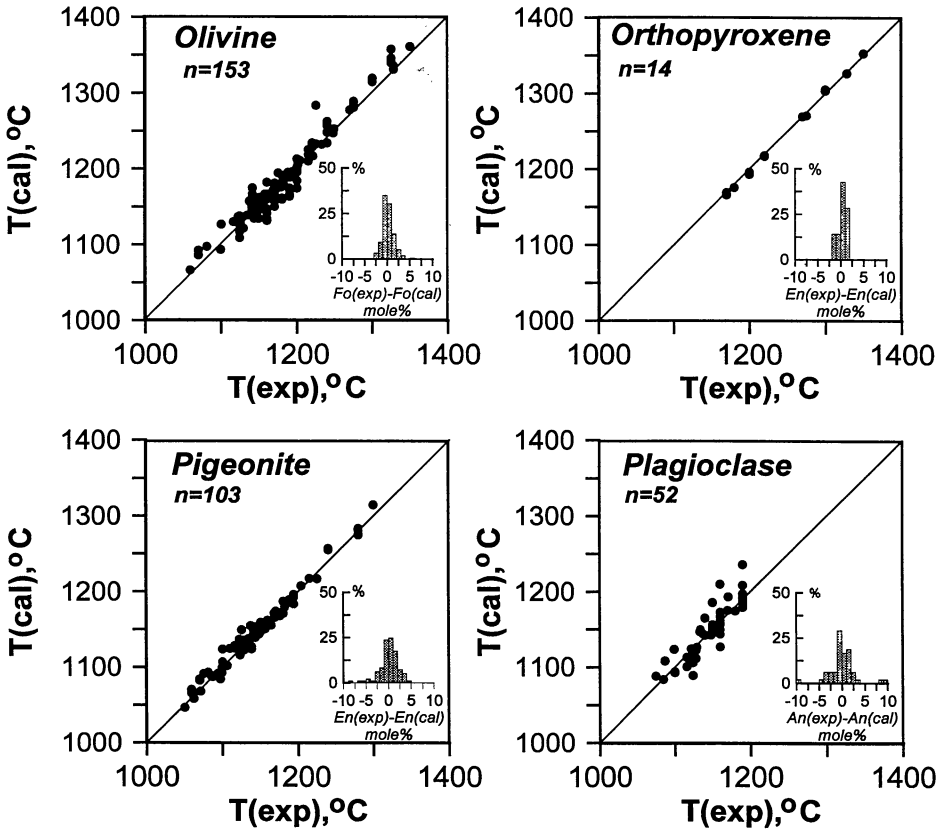

FIG. 4. Experimental *vs.* calculated temperatures for combined mineral-melt geothermometers. Liquidus temperature for each mineral is calculated for the given experimental melt composition. The compositions of minerals equilibrated with the melts were calculated simultaneously. The histograms show differences (in rel% of total number of runs) between measured and calculated contents of end members.

where $a_{FeO(L)}$ and $a_{Fe(Met)}$ denote activities of FeO in the liquid and Fe in the metal, respectively. For an activity of Fe in metal phase equal to 1, rearrangement of Eq. (11) gives an expression for the solubility of FeO in silicate melts:

$$\log X_{FeO(L)} = 0.5 \log f_{O_2} + \log K(T) - \log \gamma_{FeO(L)} \quad \text{Eq. (13)}$$

where $X_{FeO(L)}$ and $\gamma_{FeO(L)}$ are the concentration and activity coefficient of FeO dissolved in silicate melt, respectively.

The empirical basis for calibration of this expression is a library of 396 one-atm melting experiments that have been carried out on synthetic and natural systems. The data on equilibrium between pure Fe and silicate melts (± silicate minerals) include runs conducted in the 1150–1327 °C temperature range under controlled O fugacities of $14.5 < \log f_{O_2} < -11.0$ (Roeder, 1974; Doyle and Naldrett, 1986; Doyle, 1988). The melt compositions range from "basaltic" to "andesitic," with FeO contents varying from 6 to 60 wt%. The data set contains systems enriched both in K_2O (up to 13 wt%) and Al_2O_3 (up to 23 wt%); several experiments were conducted in magnesium-free and high-Ti systems.

The data were processed by least-squares fitting to obtain the expression

$$\log X_{FeO(L)} = k \log f_{O_2} + \frac{h}{T} + \sum d_j X_{j(L)} \quad \text{Eq. (14)}$$

where $X_{FeO(L)}$ is the concentration of ferrous Fe in the melt, X_j are the molar concentrations of seven petrogenetic oxides such as SiO_2, TiO_2, Al_2O_3, MgO, CaO, Na_2O, and K_2O, and the regression parameters k, h, and d_j account for the effects of f_{O_2}, temperature, and melt composition. The division of FeO_{tot} in melts into Fe_2O_3 and FeO species was carried out using the equation of Borisov and Shapkin (1990); the $X_{j(L)}$ values were calculated on an iron-free basis. The calculated regression parameters and their standard deviations are listed in Table 3. Note that the calculated value for k (0.51791) does not differ significantly from the theoretical value of 0.5, and the value of h is close to the reciprocal temperature slope defined for IW O buffer (Myers and Eugster, 1983).

Using the regression parameters (Table 3), Eq. (14) can be used to calculate the FeO solubility in the experimental melts used to calibrate the equation. Figure 5 compares the experimental and calculated FeO contents. One can see that the large range of $\log X_{FeO}$ values (0.58–1.68) for melts in the initial data set are reproduced with the good accuracy of ±0.035, which corresponds to an accuracy of ~1 mol% FeO. The calculations can be also inverted to calculate the temperature of metal crystallization from silicate melts with a given FeO content:

TABLE 3. The regression constants to Eqs. (11,12) describing saturation of silicate melts with Fe.

Parameter	Constant	Std deviation
k ($\lg f_{O_2}$)	0.51791	0.005602
h (1/T)	11623.16	208.19
d (SiO_2)	0.00287	0.00102
d (TiO_2)	0.01019	0.00147
d (Al_2O_3)	0.00174	0.00179
d (MgO)	0.00143	0.00106
d (CaO)	-0.00433	0.00145
d (Na_2O)	-0.01816	0.00375
d (K_2O)	-0.03878	0.00244

$$T = \frac{11623.16}{[\log X_{FeO(L)} - 0.51791 \log f_{O_2} - \sum d_j X_{j(L)}]} \quad \text{Eq. (15)}$$

Reversal calculations for the initial 396 melts show that for 76% of the data the difference between the experimental and calculated temperatures (Fig. 5) is <10 °C, with the average deviation being ±7.4 °C. In fact, Eq. (15) describes the liquidus surface of Fe-metal in silicate systems and can be easily incorporated into the METEOMOD phase equilibria model to calculate Fe precipitation from melts. This provides an opportunity for the quantitative study of metal crystallization, paying special attention to mineralogical and chemical consequences of the presence of metal phase in meteoritic igneous systems.

APPLICATION OF THE METEOMOD PROGRAM

METEOMOD: Structure, Opportunities and Limitations

We noted earlier that the METEOMOD program inherits the general algorithm of the LUNAMAG and COMAGMAT programs. However, incorporation of the new regression parameters of the mineral-melt geothermometers (Table 2) and of metal-melt equilibrium (Table 3) required some modifications both in the algorithm and in the set of input parameters. The combination of input files and new computation algorithm constitutes the METEOMOD program.

The input parameters include (1) the increment in crystallization, which now may vary from 0.5 to 2 mol%; (2) one of 12 f_{O_2} buffers routinely used in petrology, such as IW, QFM, NNO, *etc.*; (3) a shift from the buffer in log units (*e.g.* IW–1.5); (4) whether the crystallization trajectory is equilibrium or fractional; (5) the terminal degree of crystallization, which may be as high as 98 mol%; (6) the concentrations of major oxides in the melt: SiO_2, TiO_2, Al_2O_3, FeO, MnO, MgO, CaO, Na_2O, K_2O, P_2O_5; (7) choice of a set of minor and trace elements to be included (one includes Mn, Ni, Co, Cr, Sc, V, Sr, Ba, Rb and Cu; the other consists of ten rare-earth-elements); (8) the number of initial compositions that are to be modeled in a single computation run.

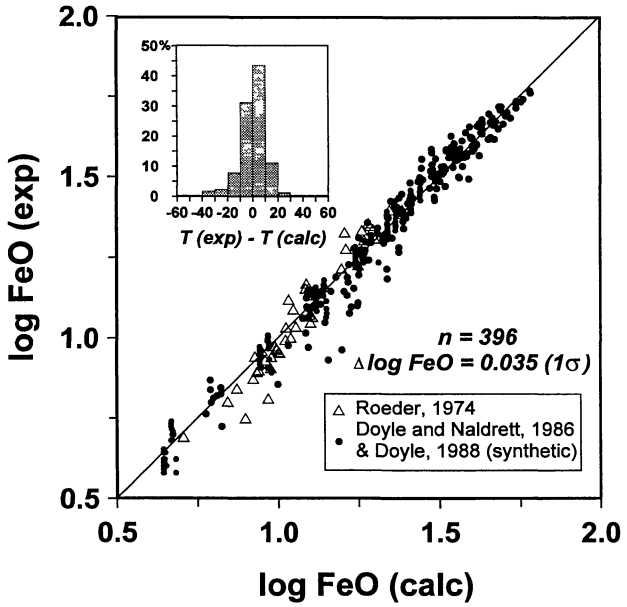

FIG. 5. Experimental *vs.* calculated solubility of FeO in synthetic and natural silicate melts equilibrated with metal (pure Fe). The values of log FeO(exp) were calculated from Eq. (14), based on the regression parameters of Table 3. The histogram shows differences (in rel% of total number of runs) between measured and calculated (from the Eq. 15) temperatures.

Modeling of crystallization starts from a completely molten system (0% solids) and proceeds by the given increment through consecutive increases in crystallization degree. For each crystallization degree, a complete set of data on the equilibrium among melt and minerals is calculated. This set includes the temperature, proportions of minerals and melt, chemical composition of the melt and contents of end members in mineral solid solutions, and concentrations of minor and trace elements in each phase. The output consists of a series of tables that list all these data as a function of the crystallization degree and the equilibrium temperature.

The present version of METEOMOD is calibrated to calculate equilibrium phase relations in partially molten volatile-depleted and iron-rich systems ranging in composition from lunar basalts to chondrites at low melting degree. The crystallization temperatures of minerals and their compositions are typically calculated with accuracies of 10–15 °C and 1–2 mol%, respectively. The uncertainties in major oxides contents of melts coexisting with crystalline phases are expected to be $<\pm 0.5$ wt%. This level of accuracy can be achieved only in the modeling of phase relations in partially molten systems whose melt compositions fall into the range of experimental melts (Table 1). Melt compositions outside the range listed in Table 1 will generally diminish the accuracy of calculated phase equilibria. The program allows the introduction of additional corrections for minor deviations in melt compositions in order to improve the fit to specific experimental data (*e.g.*, experiments on Martian basalts). In order to model phase equilibria in systems with melt compositions deviating significantly from those in Table 1, the mineral-melt geothermometers would need to be recalibrated on an appropriate database.

Simulating Equilibrium Crystallization of Ordinary Chondrites

To demonstrate application of the METEOMOD program to meteorites, we calculated the equilibrium crystallization of a chondritic melt for several redox conditions. The initial melt composition shown in Table 4 was close to that of the St. Severin ordinary chondrite minus 90% of its volatiles (Na_2O, P_2O_5, S) and all Ni and Cr. The volatile contents were decreased intentionally in order to approximate better the composition of the melts studied in experiments by Jurewicz *et al.* (1995). Nickel and Cr are treated in the present version of METEOMOD as trace elements, so they have no effect on calculated phase relations.

Calculation of equilibrium crystallization was carried out at 1 atm total pressure, for 1 mol% increments of solids, and at two different values of f_{O_2}, corresponding to the iron-wüstite buffer (log f_{O_2} = IW) and to 2 log units below that (log f_{O_2} = IW–2). The maximum crystallization degrees modeled were 89 mol%, which corresponds to minimum melting degrees of the model system of 11.6 and 11.2 wt% at log f_{O_2} = IW and log f_{O_2} = IW–2, respectively. The calculated crystallization sequences are shown in Fig. 6; chemical trends of the model residual melts are plotted in the generalized phase diagram for meteoritic systems (Fig. 7).

The major difference between the two calculated chemical trends (Figs. 6, 7) is caused by the behavior of the metal phase. At log f_{O_2} = IW, metal does not crystallize, whereas at log f_{O_2} = IW–2 the crystallization of metal begins before that of silicate minerals. This changes the phase diagram of the modeled chondritic system significantly. It has the most pronounced effect on the proportions of olivine and orthopyroxene among solids. Figure 6 clearly shows that under more reduced conditions (log f_{O_2} = IW–2) the initial crystallization temperature of orthopyroxene is >100 °C higher than that at log f_{O_2} = IW. This means that the orthopyroxene stability field enlarges as f_{O_2} decreases. The cause of this is early metal precipitation, which results in the complementary enrichment of the residual melt in SiO_2 and in the increase of mg# of the silicate portion of the system modeled. Similar effects of metal precipitation on the position of phase boundaries in the OLIV-PLAG-QTZ diagram for basaltic achondrites have been discussed previously by Ariskin *et al.* (1993a).

The OLIV-PLAG-QTZ diagram (Fig. 7) shows that the calculated chemical trends of residual melts match the experimental olivine-orthopyroxene peritectics quite well. This could not be straightforwardly predicted, because the calculation of real mineral proportions in the reaction Ol + L = Op ± Pl is one of the most difficult problems of computer modeling. In our case, the good match between the calculated and experimental peritectics provides additional evidence for the correct calibration of the basic mineral-melt geothermometers and the effectiveness of the METEOMOD algorithm.

TABLE 4. The effect of O fugacity on the experimental and calculated silicate melts and phase equilibria.

Component, wt%	Saint Severin Chondrite		Experiment: Jurewicz *et al.*, 1995	Calculated: this work	Experiment: Jurewicz *et al.*, 1995	Calculated: this work
	Bulk (Jurewicz *et al.*, 1995)	Adopted (this work)	IW+2, 1210 °C *Ol + Op + L*	IW, 1202.8 °C *Ol + Op + L* F_{melt} = 20.0%	IW-1, 1200 °C *Ol + Op + L + Metal*	IW-2, 1212.1 °C, *Ol + Op + Pl + L + Metal* F_{melt} = 12.2%
SiO_2	40.60	42.60	50.60	51.88	50.70	51.66
TiO_2	0.11	0.11	0.38	0.51	0.47	0.81
Al_2O_3	2.37	2.45	9.96	11.90	13.00	18.35
FeO	25.90	26.83	21.90	19.73	17.80	9.94
MnO	0.32	0.33	0.28	0.30	0.32	0.31
MgO	25.20	26.10	7.67	7.27	7.31	8.78
CaO	1.92	1.99	7.92	7.79	8.39	9.08
Na_2O	1.00	0.10	0.31	0.52	0.69	0.89
P_2O_5	0.22	0.02	0.11	0.10	0.52	0.19
NiO	1.34	–	0.18	–	0.04	–
Cr_2O_3	0.58	–	0.14	–	0.38	–
Total	99.56	100.0	99.45	100.0	99.62	100.0
Mg/(Mg + Fe)	0.634	0.634	0.384	0.396	0.423	0.612
Ca/(Ca + Al)	0.424	0.425	0.420	0.373	0.370	0.310
K_d(*Ol-L*)	–	–	0.34	0.358	0.350	0.335

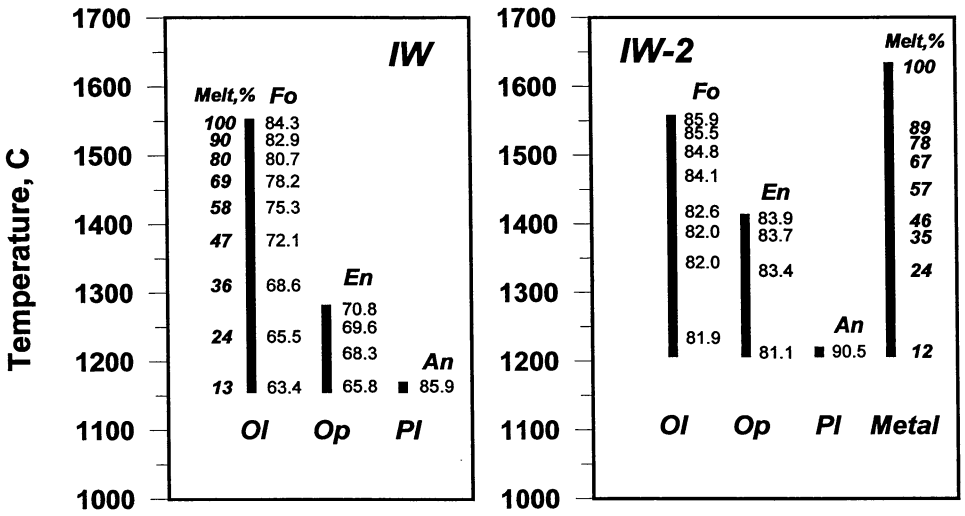

FIG. 6. Crystallization sequences of melts of chondritic composition (volatile-depleted St. Severin LL chondrite) at two O fugacities. Numbers in the plots show composition of minerals (forsterite, enstatite, anorthite) at different degrees of melting (melt percent).

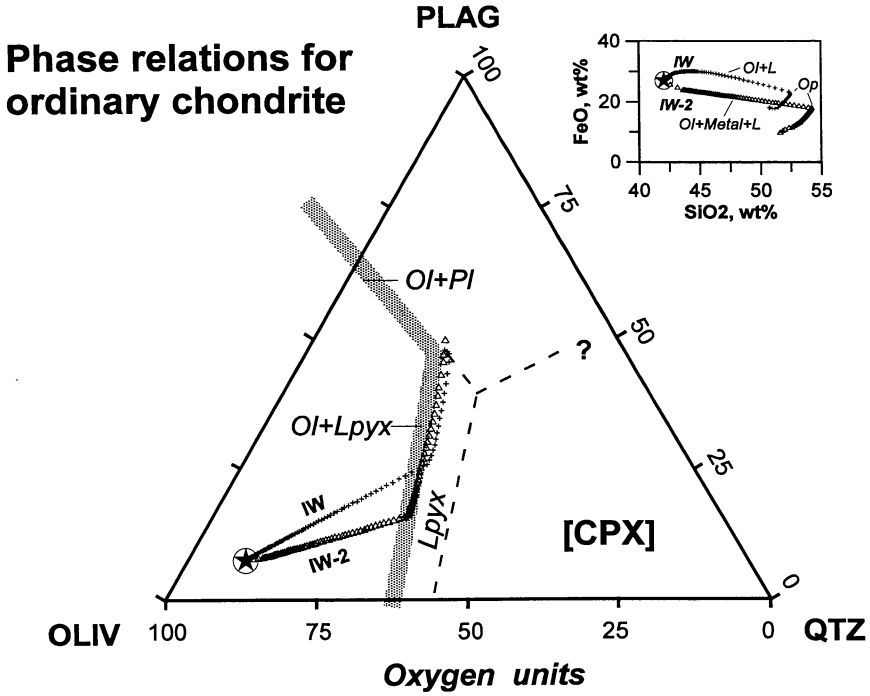

FIG. 7. Compositional trends in melts produced by modelled melting/crystallization of volatile-depleted St. Severin LL chondrite at two O fugacities. Model compositions of melts and solids are projected from the CPX component by the technique of Tormey *et al.* (1987). The star denotes initial composition (Table 4). Shaded bands show olivine–low-ca pyroxene and olivine-plagioclase peritectics. Low-Ca pyroxene–quartz, Low-Ca pyroxene–plagioclase, and plagioclase-quartz peritectics are marked by dashed lines. The inset shows that the melt produced at lower f_{O_2} becomes enriched in SiO_2 as a result of crystallization of Fe metal.

Comments on the Problem of Origin of Asteroidal Basalts

The results of the calculations presented above have a direct implication to the origin of eucrites, diogenites, and howardites. The melting experiments on chondrites and their synthetic equivalents have shown that partial melting of a volatile-depleted chondritic precursor at reduced conditions (IW–1 and below) can produce SiO_2-enriched melts compositionally similar to eucrites and suggested primary diogenitic magmas (Jurewicz *et al.*, 1993, 1995). The results of our calculation are consistent with this conclusion.

Table 4 compares the compositions of experimental and calculated melts produced at near-liquidus temperatures of the St. Severin chondrite (1200–1212 °C) for different redox conditions. Both sets of data show a depletion of residual melts in FeO and an enrichment in Al_2O_3 as O fugacity decreases. This means that the redox condition accompanying partial melting of parent body interiors may be a major factor affecting the compositions of primary magmas, including the magnesium percent of olivines and othopyroxenes that would crystallize from them upon cooling.

These effects can be modeled quantitatively using the METEOMOD program.

CONCLUSION

The METEOMOD computer program provides an opportunity to apply modern methods of experimental petrology and the computer modeling of igneous systems to meteorite studies. The present version of METEOMOD is a tool for the numerical modeling of equilibrium phase relations in partially molten high-Fe^{2+} igneous systems compositionally similar to ordinary chondrites and basaltic achondrites under various redox conditions. The program calculates the crystallization temperatures of olivine, orthopyroxene, pigeonite, augite, plagioclase, and metallic iron (100% Fe), and the proportions of major end members in these mineral solid solutions, with accuracies of ±10–15 °C and ±1–2 mol%, respectively. Future development of METEOMOD will allow for incorporation of the chromian spinel-melt geothermometer (Ariskin and Nikolaev, 1996) and the equation for Ni solubility in both metal and silicate melt (Borisov and Ariskin, 1996) in a single program.

The present version of METEOMOD program may be provided upon request sent to the senior author at ariskin@glas.apc.org.

Acknowledgments–We are very grateful to Dr. J. A. Wood and Dr. O. I. Yakovlev for invaluable discussions and help during preparation of the manuscript. Constructive and helpful reviews by J. H. Jones, D. M. Shaw and A. Woronow are greatly appreciated. This work was supported by Russian Foundation of Basic Research Grant #96-05-64231 (to A. A. A.) and NASA Grant NAGW 3451 (to J. A. W.).

Editorial handling: D. Shaw

NOTES

1. *Ol* = olivine, *Au* = augite, *Op* = orthopyroxene, *Pg* = pigeonite, *LPyx* = low-Ca pyroxene (*Op* or *Pg*), *Pl* = plagioclase, *Sp* = spinel, *Met* = metal, *Fo* = forsterite, *Fa* = fayalite, *En* = enstatite, *Fs* = ferrosilite, *Wo* = wollastonite, *An* = anorthite, *Ab* = albite, *Qtz* = quartz
2. At the development of combined pyroxene-melt geothermometers, we took into account the partitioning of alumina into pyroxenes, using the following average calculated values of single molar distribution coefficients D_{Al} : 0.057 ± 0.020 for *Op*, 0.115 ± 0.033 for *Pg*, and 0.241 ± 0.112 for *Au*.

REFERENCES

ARISKIN A. A. AND NIKOLAEV G. S. (1996) An empirical model for the calculation of spinel-melt equilibria in mafic igneous systems at atmospheric pressure: 1. Chromian spinels. *Contrib. Mineral. Petrol.* **123,** 282–292

ARISKIN A. A., BARMINA G. S. AND FRENKEL M. YA. (1987) Computer simulation of basalt magma crystallization at a fixed oxygen fugacity. *Geochem. Intern.* **24,** 85–98.

ARISKIN A. A., BARMINA G. S. AND FRENKEL M. YA. (1991) Simulation of the crystallization of lunar-basalt melts. *Geochem. Intern.* **28,** 92–100.

ARISKIN A. A., BORISOV A. A. AND BARMINA G. S. (1993a) Simulating iron-silicate melt equilibrium in basaltic systems. *Geochem. Intern.* **30,** 13–22.

ARISKIN A. A., FRENKEL M. YA., BARMINA G. S. AND NIELSEN R. L. (1993b) COMAGMAT: A Fortran program to model magma differentiation processes. *Comp. Geosci.* **19,** 1155–1170.

ARISKIN A. A., BARMINA G. S., MESHALKIN S. S., NIKOLAEV G. S. AND ALMEEV R. R. (1996) INFOREX-3.0: A database on experimental studies of phase equilibria in igneous rocks and synthetic systems. II. Data description and petrological applications. *Comp. Geosci.* (in press).

BARTELS K. S. AND GROVE T. L. (1991) High-pressure experiments on magnesian eucrite compositions: Constrains on magmatic processes in the eucrite parent body. *Proc. Lunar Planet. Sci. Conf.* **21th,** 351–365.

BORISOV A. A. AND ARISKIN A. A. (1996) Fe and Ni solubility in silicate melts equilibrated with metal (abstract). *Lunar Planet. Sci.* **27,** 133–134

BORISOV A. A. AND SHAPKIN A. I. (1990) A new empirical equation relating Fe^{3+}/Fe^{2+} in magmas to their composition, oxygen fugacity, and temperature. *Geochem. Intern.* **27,** 111–116.

DOYLE C. D. (1988) Prediction of the activity of FeO in multicomponent magma from known values in [SiO_2-$KAlO_2$-$CaAl_2Si_2O_8$]-FeO liquids. *Geochim. Cosmochim. Acta* **52,** 1827–1834.

DOYLE C. D. AND NALDRETT A. J. (1986) Ideal mixing of divalent cations in mafic magma and its effect on the solution of ferrous oxide. *Geochim. Cosmochim. Acta* **50,** 435–443.

FRENKEL M. YA. AND ARISKIN A. A. (1984) A computer algorithm for equilibration in a crystallizing basalt magma. *Geochem. Intern.* **21,** 63–73.

GAFFEY M. J., BURBINE T. H. AND BINZEL R. P. (1993) Asteroid spectroscopy: Progress and perspectives. *Meteoritics* **28,** 161–187

JUREWICZ A. J. G., MITTLEFEHLDT D. W. AND JONES J. H. (1991). Partial melting of the Allende (CV3) meteorite: Implications for origins of basaltic meteorites. *Science* **252,** 695–698.

JUREWICZ A. J. G., MITTLEFEHLDT D. W. AND JONES J. H. (1993) Experimental partial melting of the Allende (CV) and Murchison (CM) chondrites and the origin of asteroidal basalts. *Geochim. Cosmochim. Acta* **57,** 2123–2139.

JUREWICZ A. J. G., MITTLEFEHLDT D. W. AND JONES J. H. (1995) Experimental partial melting of the St. Severin (LL) and Lost City (H) chondrites. *Geochim. Cosmochim. Acta* **59,** 391–408.

GHIORSO M. S. (1985) Chemical mass transfer in magmatic processes I. Thermodynamic relations and numerical algorithms. *Contrib. Mineral. Petrol.* **90,** 107–120

GHIORSO M. S. AND SACK R. O. (1995) Chemical mass transfer in magmatic processes IV. A revised and internally consistent thermodynamic model for the interpolation and extrapolation of liquid-solid equilibria in magmatic systems at elevated temperatures and pressures. *Contrib. Mineral. Petrol.* **119,** 197–212.

LONGHI J. (1987) On the connection between mare basalts and picritic volcanic glasses. Experimental petrology and petrogenesis of mare volcanics. *J. Geophys. Res.* **92,** E349–E360.

LONGHI J. (1991) Comparative liquidus equilibria of hypersthene-normative basalts at low pressure. *Amer. Mineral.* **76,** 785–800.

LONGHI J. AND PAN V. (1989) The parent magma of the SNC meteorites. *Proc. Lunar Planet. Sci. Conf.* **19th,** 451–464.

LUGMAIR G. W., SHUKOLYUKOV A. AND MACISAAC CH. (1996) Radial heterogeneity of ^{53}Mn in the early solar system and the place of origin of ordinary chondrites (abstract). *Lunar Planet. Sci.*. **27,** 37–38

MESHALKIN S. S. AND ARISKIN A. A. (1996) INFOREX-3.0: A database on experimental studies of phase equilibria in igneous rocks and synthetic systems. I. Datafile and management system structure. *Comp. Geosci.* (in press).

MYERS J. AND EUGSTER H. P. (1983) The system Fe-Si-O: Oxygen buffer calibrations to 1,500K. *Contrib. Mineral. Petrol.* **82,** 75–90.

NAZAROV M. A. AND ARISKIN A. A. (1993) The Erevan howardite: Petrology of glassy clasts and mineral chemistry (abstract). *Lunar Planet. Sci.* **24,** 1049–1050.

NIELSEN R. L. AND DUNGAN M. A. (1983) Low-pressure mineral-melt equilibria in natural anhydrous mafic systems. *Contrib. Mineral. Petrol.* **84,** 310–326.

NIELSEN R. L. (1990) Simulation of igneous differentiation processes. *Reviews in Mineralogy* **24,** 63–105.

PETAEV M. I., ARISKIN A. A. AND WOOD J. A. (1994a). Numerical model of genetic link between Acapulco and Y791493 primitive achondrites. I. Phase equilibria and major element constraints chemistry (abstract). *Lunar Planet. Sci.* **25,** 1071–1072.

PETAEV M. I., ARISKIN A. A. AND WOOD J. A. (1994b). Numerical model of genetic link between Acapulco and Y791493 primitive achondrites. II. Implications to the origin of acapulcoites and lodranites (abstract). *Lunar Planet. Sci.* **25,** 1073–1074.

PETAEV M. I., BARSUKOVA L. D., LIPSCHUTZ M. E., WANG M.-S., ARISKIN A. A., CLAYTON R. N. AND MAYEDA T. K. (1994c). The Divnoe mete-orite: Petrology, chemistry, oxygen isotopes and origin. *Meteoritics* **29,** 182–199.

ROEDER P. L. (1974) Activity of iron and olivine solubility in basaltic liquids. *Earth Planet. Sci. Lett.* **23,** 397–410.

SACK R. O., GHIORSO M. S., WANG M.-S. AND LIPSCHUTZ M. E. (1994) Igneous inclusions from ordinary chondrites: High temperature cumulates and a shock melt. *J. Geophys. Res.* **99,** E26029–26044.

STOLPER E. (1977) Experimental petrology of eucritic meteorites. *Geochim. Cosmochim. Acta* **41,** 587–611.

STOLPER E. AND MCSWEEN H. Y., JR. (1979) Petrology and origin of the shergottite meteorites. *Geochim. Cosmochim. Acta* **43,** 1475–1498.

TORMEY D. R., GROVE T. L. AND BRYAN W. B. (1987) Experimental petrology of normal MORB near the Kane Fracture Zone: 22°–25° N, mid-Atlantic ridge. *Contrib. Mineral. Petrol.* **96,** 121–139.

WEAVER J. S. AND LANGMUIR C. H. (1990) Calculation of phase equilibrium in mineral-melt systems. *Comp. Geosci.* **16,** 1–19.